J Syst Eng (1994)4:60–69

Journal of Systems Engineering

Characterisation of a Three Degree-of-Freedom Variable Reluctance Spherical Motor

Zhi Zhou and Kok-Meng Lee

The George W. Woodruff School of Mechanical Engineering, Georgia Institute of Technology, Atlanta, Georgia 30332-0405, USA

This paper presents a practical approach to characterise and optimise a ball-joint-like three degree-of-freedom (DOF) variable reluctance (VR) spherical motor which has potential applications as a direct-drive robotic wrist. Unlike the conventional single-axis (1-DOF) motor, the 3-DOF VR spherical motor is characterised by its multiple independent inputs and the direction-varying and orientation-dependent torque output. The design and control of 3-DOF spherical motors are significantly different from that of 1-DOF actuators. In order to characterise the torque of a 3-DOF spherical motor, a maximum torque-to-input power ratio is derived to describe explicitly the relationship between the torque output and the electrical power input. This relationship, along with the presentation of the numerical techniques, provides an effective means to characterise and optimise 3-DOF spherical motors, which is essential to integrated design and control of the motors. Several typical applications are illustrated here, including the estimation of the maximum payload, proof of the non-singularity property, choice of an objective function for design optimisation, and determination of the characteristic orientation where a global design optimisation can be accomplished. Results showed good agreement between the theoretical and actual maximum torque outputs. Some new and unique concepts for 3-DOF devices are also addressed in the paper.

Keywords: Variable reluctance; Spherical motor; Torque characterisation; Design optimisation

1. Introduction

The ability to characterise the specifications of an actuator is essential in design and control strategy development. There are well developed and widely accepted specifications and associated theories for characterisation of 1-DOF motors, which include the rated maximum torque output. Maximising output torque capacity has well been recognised by researchers as one of the major objectives in designing 3-DOF direct-drive actuators. A properly designed actuator (motor) with maximum torque output capacity will improve the starting characteristics, and hence the system performance, by effectively overcoming system inertia and unexpected load.

The goal of maximising torque output can be achieved by hardware (structure and parameters) design optimisation and by software (control algorithms) development. One typical example in designing 1-DOF motors is to choose the geometric parameters so that the torque constant (torque-to-current ratio) is maximised. The maximum torque output of a 1-DOF motor can be described by a relatively simple and explicit relationship between the output toruqe and the input. Most conventional 1-DOF motors generally have only one independent input, and the torque output is in a constant, specific direction. However, 3-DOF ball-joint-like motors usually have multiple independent inputs, and the output torque is direction-varying and

Final manuscript received 18 April 1994

Correspondence and offprint requests to: K.-M. Lee, The George W. Woodruff School of Mechanical Engineering, Georgia Institute of Technology, Atlanta, Georgia 30332-0405, USA.

circuit to saturate. Therefore, the actual torque output is lower than the predicted value.

To understand fully how the maximum torque-to-input power ratio varies with the torque direction variables, a torque profile, namely a surface plot of $T_{sup}/\|\mathbf{u}\|^2$ in terms of φ and ϑ, is plotted at the characteristic orientation based on the following formula:

$$\frac{T_{sup}}{\|\mathbf{u}\|^2} = \min_{\mathbf{T}}\left\{\frac{|\lambda_3^*|}{2|\cos\varphi|}, \frac{|\lambda_2^*|}{2|\sin\varphi\sin\vartheta|}, \frac{|\lambda_1^*|}{2|\sin\varphi\cos\vartheta|}\right\}$$

where $\lambda_i^*(i = 1,2,3)$ is defined by Eq. (24), and $\mathbf{A}_i$ is the matrix at the characteristic orientation.

One may observe from the plot (Fig. 5) that the minimum value of $T_{sup}/\|\mathbf{u}\|^2$, corresponding to the payload-to-input power ratio, occurs at $\varphi = 0$ or π. The plot is symmetrical about $\varphi = \pi/2$ and $\vartheta = \pi/2$, which reflects the symmetrical structure of the motor. Furthermore, the plot is small-valued and flat where φ is away from $\pi/2$, but relatively steep in the adjacent vicinity of $\pi/2$. This indicates that the motor has a bigger output torque potential in that region. The torque profile gives an overall insight into the output torque capacity, which is very useful and important to future designs.

6. Conclusions

This paper has presented a practical approach to characterise and optimise a 3-DOF VR spherical motor. The formula derived for predicting the maximum torque provided an effective means to determine the characteristic orientation analytically and to prove numerically the non-singularity property without calculating the exact maximum torque output, a solution of a non-linear optimisation problem. This, along with the numerical techniques developed in the paper, greatly reduced the computation. Although the actual maximum torque output can be numerically calculated by solving the non-linear optimisation problem, the maximum torque output at the characteristic orientation was shown to be close to the theoretical estimate by using the anlaytical maximum torque formula. The formula also offered a more desirable objective function for design optimisation. Several unique concepts developed in this paper for 3-DOF actuators are summarised as: (1) torque direction variables, (2) characteristic orientation, (3) global design optimisation, and (4) maximum torque-to-input power ratio. The results of this work formed an essential basis for further development. The experimental implementation of the results is currently being investigated.

References

1. Lee K-M, Wang XA, Wang NH. Dynamic modeling and control of a ball-joint-like variable-reluctance spherical motor. In: Symposium on mechatronics, ASME winter annual meeting, New Orleans, November 1993, pp 71–79
2. Roth RB. An experimental investigation and optimization of a variable reluctance spherical motor. Ph. D. Thesis, Mechanical Engineering, Georgia Tech, Atlanta, GA, 1992
3. Horn, RA, Johnson CR. Matrix analysis. Cambridge University Press, 1991, pp 176–180
4. Lee K-M, Zhou Z, Wang NH. A practical optimal control strategy for a variable reluctance spherical motor. In: Symposium on mechatronics, ASME winter annual meeting, New Orleans, November 1993, pp 39–47
5. Abadie J, Carpentier J. Generalization of the Wolfe reduced gradient method to case of nonlinear constraints. In: Optimization edited by Fletcher R, Academic Press, 1969, pp 37–47

orientation (position)-dependent. These unique features make the characterisation of 3-DOF motors significantly different from and more difficult than the 1-DOF case.

In order to advance the development of 3-DOF actuators, specifications and associated theories for characterising 3-DOF motors are necessary. We present here a new approach to address some fundamental issues in design and control of a 3-DOF variable reluctance (VR) spherical motor. The major contributions of this paper are summarised as follows: (1) The paper derives analytically an explicit formula for predicting the maximum torque output of a 3-DOF VR spherical motor. (2) The results of this analytical investigation form an essential basis for integrated design/control and characterisation of 3-DOF VR spherical motors. (3) Methods of using these results have been illustrated to estimate the maximum output torque capacity (payload) of a VR spherical motor over the entire workspace, to verify numerically the non-singularity property, and to determine the characteristic orientation upon which a global design optimisation can be accomplished. (4) The paper explores and develops some unique concepts of 3-DOF actuators as compared to 1-DOF devices.

The remainder of the paper has five sections. Section 2 briefly describes the VR spherical motor. Section 3 presents first a spherical coordinate representation of the constraints and a maximum torque formulation for design and control of the VR spherical motor. An analytical maximum torque formula is then developed to relate the maximum torque output potential to the electrical power input of the motor. Section 4 illustrates four typical applications of the maximum torque formula derived in Section 3; namely, payload evaluation, numerical verification of non-singularity property, characteristic (global) design optimisation, and optimal solution to the maximum torque formulation for control strategy development. Numerical results and discussion are given in Section 5. Conclusions are drawn in Section 6.

2. A VR Spherical Motor

A number of mechanisms have been proposed in designing unusual three DOF direct-drive devices. Among the developments is a ball-joint-like VR spherical motor that combines three DOF rotation in a single joint. As shown in Figs 1 and 2, a prototype design of the VR spherical motor consists of four basic assemblies: (1) a solid spherical rotor, (2) a hollow spherical stator, (3) a bearing system, and (4) an orientation measurement system. The rotor consists of n iron poles embedded in a round, smooth sphere following the pattern of a regular polygon. The rotor poles connected at the rotor core provide a return path of magnetic flux. The stator consists of a hollow sphere constructed of iron and m stator poles with coils wound on ferromagnetic cores. The stator sphere provides a magnetic flux path for linking stator poles and serves as a mechanical structure for supporting the stator poles, transfer bearings, and orientation measurement system. The stator poles are evenly located on the inner stator surface and at the vertices of a regular polygon. The stator and rotor spheres are concentric and are supported one on the other by bearings in the airgap. The bearings are threaded externally to the stator such that a constant airgap can be calibrated between the poles of the rotor and the stator. The orientation measurement system consists of two arc-shaped guides, one sliding block, and three encoders. The two guides are mounted orthogonally on bearing pins attached to the outside stator shell. The sliding block is confined to move along the slot of the top guide. A hole in the sliding block allows the output shaft to extend through.

Once currents are applied to the stator coils, magnetic fluxes flow through the magnetic circuit and create magnetic energy in the airgap. The created energy is a function of the currents and the reluctance of the airgap between the rotor and stator poles. The motion of the rotor is thus generated as the magnetic system tends to minimise the energy stored in the airgaps. The reluctance of the airgap is a function of the relative position between the rotor and the stator. It varies as the rotor moves, hence the name 'variable reluctance' motor.

The torque model that describes the electromagnetic interaction of the VR spherical motor has been derived and experimentally verified by Lee *et al.* [1] using the energy conservation principle. The model has been expressed in rotor-fixed Cartesian coordinates by the following quadratic form:

$$T_i = \frac{1}{2}\mathbf{u}^{\mathrm{T}}\mathbf{A}_i\mathbf{u} \quad (i = 1,2,3)$$

where T_i denotes the torque components acting on the rotor in the x, y, and z directions, respectively; $\mathbf{u}$ represents the control vector (magnetomotive force), and $\mathbf{A}_i$ is real-symmetric and indefinite matrix whose elements are functions of rotor orientation and airgap permeance [2].

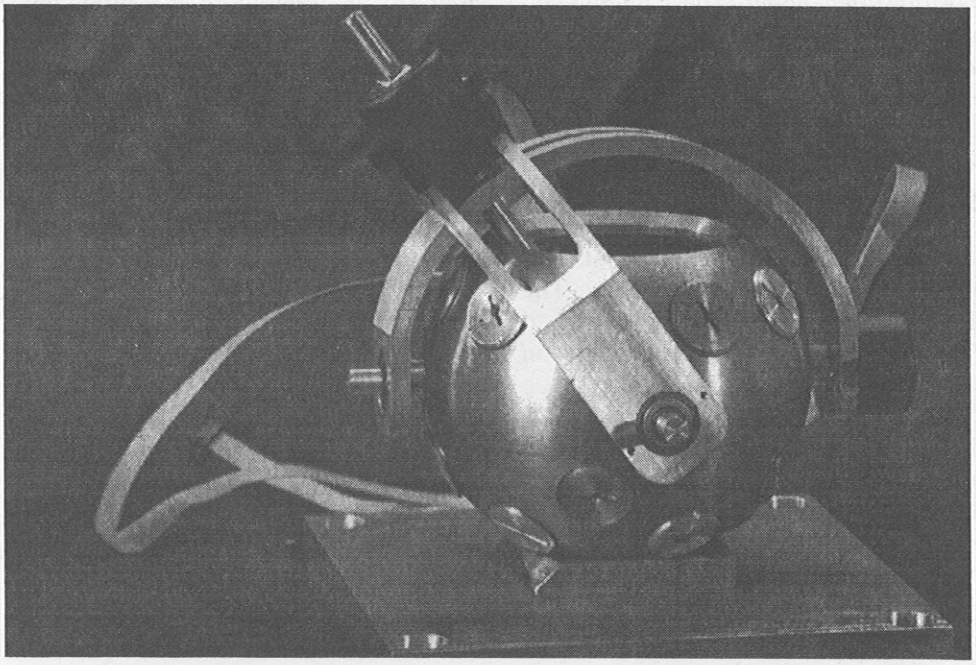

Fig. 1. A variable reluctance spherical motor prototype.

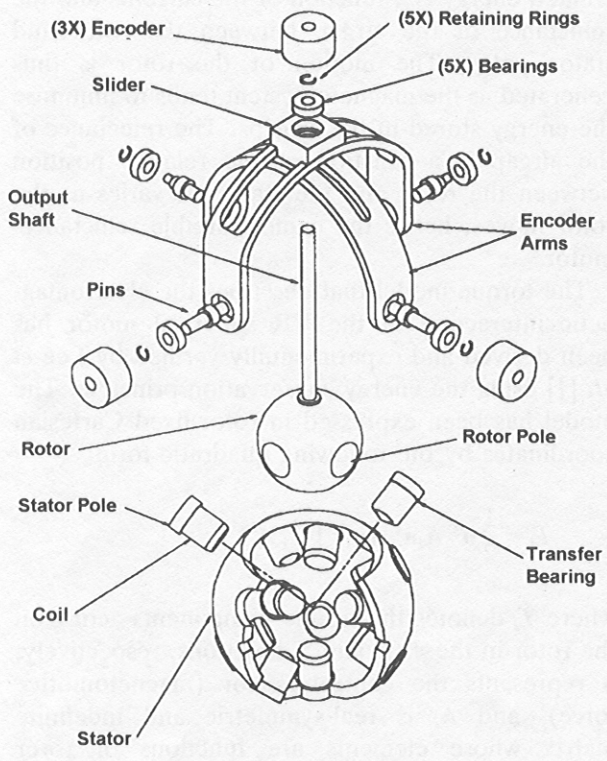

Fig. 2. An exploded assembly view of the prototype.

3. Maximum Torque Formula

The VR spherical motor has potential applications as a direct-drive device. For robotic wrist applications, it is desired that the VR spherical motor be designed with large torque-to-weight and torque-to-input power ratios. Ideally, an actuator should be able to generate an infinite torque, and should have an instantaneous dynamic response to its input. The modification of the torque characteristics of a practical actuator to approach that of the ideal actuator requires that the maximum torque output capacity be explicitly specified. To achieve this goal, a maximum torque formula derived from a maximum torque formulation of the VR spherical motor is developed in this section.

Conceptually, the maximum torque formulation for the VR spherical motor is defined here as finding a set of control inputs such that the magnitude of the generated torque in a specified direction is maximised. To formulate this optimisation problem mathematically, it is convenient to represent the constraints (specified torque direction) in spherical coordinates. This can be done by transforming the torque model in Cartesian coordinates to spherical coordinate representations first, then by taking the ratios of the torque components to eliminate the torque magnitude. Also, the objective function, namely the torque magnitude, must be expressed in spherical coordinates.

3.1. Spherical Coordinate Representation of the Torque Model

As shown in Fig. 3, an arbitrary torque can be represented by its spherical coordinates (T,ϑ,φ). We are seeking control inputs which will maximise the torque magnitude T for given ϑ and φ. From the basic trigonometry, the torque components can be written in spherical coordinates as

$$T\sin\varphi\cos\vartheta = T_1 = \frac{1}{2}\mathbf{u}^T\mathbf{A}_1\mathbf{u} \tag{1}$$

$$T\sin\varphi\sin\vartheta = T_2 = \frac{1}{2}\mathbf{u}^T\mathbf{A}_2\mathbf{u} \tag{2}$$

$$T\cos\varphi = T_3 = \frac{1}{2}\mathbf{u}^T\mathbf{A}_3\mathbf{u} \tag{3}$$

Since $T \neq 0$, suppose $T_3 \neq 0$, then from Eqs (1), (2) and (3), we have

$$\tan\varphi\cos\vartheta = \frac{T_1}{T_3} = \frac{\mathbf{u}^T\mathbf{A}_1\mathbf{u}}{\mathbf{u}^T\mathbf{A}_3\mathbf{u}} \tag{4}$$

and

$$\tan\varphi\sin\vartheta = \frac{T_2}{T_3} = \frac{\mathbf{u}^T\mathbf{A}_3\mathbf{u}}{\mathbf{u}^T\mathbf{A}_3\mathbf{u}} \tag{5}$$

By defining

$$a_3 \triangleq \tan\varphi\cos\vartheta \tag{6}$$

$$b_3 \triangleq \tan\varphi\sin\vartheta \tag{7}$$

the torque direction constraints in spherical coordinates are given by

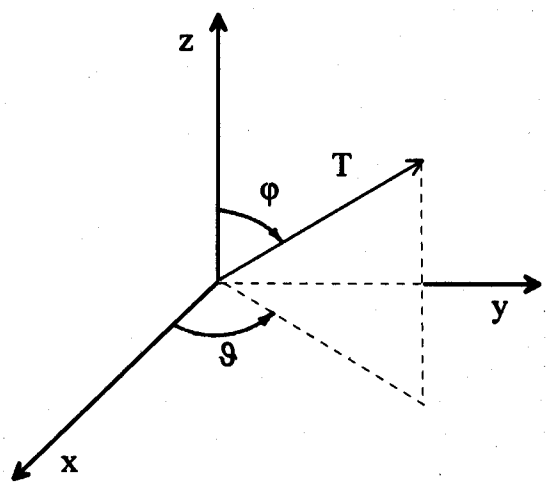

Fig. 3. Spherical coordinates.

$$\mathbf{u}^T(\mathbf{A}_1 + a_3\mathbf{A}_3)\mathbf{u} = 0 \tag{8}$$

$$\mathbf{u}^T(\mathbf{A}_2 + b_3\mathbf{A}_3)\mathbf{u} = 0 \tag{9}$$

Note that the square of the magnitude of the torque is given by

$$T^2 = T_1^2 + T_2^2 + T_3^2,$$

and that T_1 and T_2 can be expressed in terms of T_3 from Eqs (4) and (5), we have

$$T^2 = (a_3^2 + b_3^2 + 1)T_3^2.$$

Hence, by substituting T_3 from Eq. (3) to the above equation, the magnitude of the torque can be represented in spherical coordinates as

$$T = c_3\,|\mathbf{u}^T\mathbf{A}_3\mathbf{u}| \tag{10}$$

where

$$c_3 \triangleq \frac{1}{2}(a_3^2 + b_3^2 + 1)^{\frac{1}{2}} > 0 \tag{11}$$

In general, the parameter c_3 is a function of the torque direction variables, ϑ and φ, and is constant for a particular torque direction. It is worth noting that T is independent of the choice of the non-zero torque component. In other words, the assumption $T_3 \neq 0$ did not lose the generality of the formulation. However, the advantage of choosing $T_3 \neq 0$ to illustrate the derivation is that there are fewer chances that T_3 can be zero than T_1 or T_2. This is because T_3 is a function of T and φ, but not ϑ. Furthermore, $T_3 = 0$ only corresponds to $\varphi = \pi/2$ and $3\pi/2$.

3.2. Problem Statement

Based on the spherical representations of the torque magnitude and the torque direction constraints, the maximum torque formulation can now be stated as the following static constrained non-linear optimization problem.

For a specified torque direction, φ and ϑ, at a given rotor orientation, find a control input $\mathbf{u} \in \mathbf{R}^m$, which maximises the torque magnitude

$$T = 2c_3\,|T_3| = c_3\,|\mathbf{u}^T\mathbf{A}_3\mathbf{u}|,$$

subjected to the following constraints

$$\mathbf{u}^T(\mathbf{A}_1 + a_3\mathbf{A}_3)\mathbf{u} = 0 \tag{12}$$

$$\mathbf{u}^T(\mathbf{A}_2 + b_3\mathbf{A}_3)\mathbf{u} = 0 \tag{13}$$

$$\mathbf{u}^T\mathbf{u} \leq P \tag{14}$$

where a_3, b_3, and c_3 are defined by Eqs (6), (7), and (11), and P is the limit of $\mathbf{u}^T\mathbf{u}$ which is directly proportional to the consumed input power. In the

following discussions, $\mathbf{u}^T\mathbf{u}$ will be referred to as the consumed input power of the VR spherical motor without loss of generality. It is worth noting that the constraint given by Eq. (14) is equivalent to $|u_i| \leq U_{\max}$ if $P = (U_{\max}/|u_i|_{\max})^2$, where

$$|u_i|_{\max} = \max_{\mathbf{u}^T\mathbf{u}=1} |u_i|$$

3.3. Maximum Torque Formula

To achieve an isotropic torque property, the VR spherical motor has been designed to generate an arbitrary torque (below certain limit) in any direction at any rotor orientation, which means mathematically that $\mathbf{A}_i$ (i = 1,2,3) is indefinite, namely, $\lambda_{\min}(\mathbf{A}_i) < 0$, and $\lambda_{\max}(\mathbf{A}_i) > 0$.

Since $\mathbf{A}_i$ (i = 1,2,3) is real-symmetric (Hermitian), by the Rayleigh–Ritz theorem [3]

$$\lambda_{\min}(\mathbf{A}_2)\|\mathbf{u}\|^2 \leq \mathbf{u}^T\mathbf{A}_3\mathbf{u} \leq \lambda_{\max}(\mathbf{A}_3)\|\mathbf{u}\|^2 \qquad (15)$$

Two cases with different signs of the third torque component T_3 are discussed as follows.

Case I: $T_3 > 0$, or $\mathbf{u}^T\mathbf{A}_3\mathbf{u} > 0$. Since $\lambda_{\min}(\mathbf{A}_i) < 0$, the left-inequality of (15) always holds. From Eq. (10) and the right-inequality of (15), we have

$$T \leq c_3\lambda_{\max}(\mathbf{A}_3)\|\mathbf{u}\|^2$$

Therefore,

$$T_{\sup}|_{T_3>0} = c_3\lambda_{\max}(\mathbf{A}_3)\|\mathbf{u}\|^2 \qquad (16)$$

where $T_{\sup} \triangleq \sup T$ is the superior limit of the torque output, which represents the maximum torque output potential of the VR spherical motor.

Case II: $T_3 < 0$, or $\mathbf{u}^T\mathbf{A}_3\mathbf{u} < 0$. Notice that $\lambda_{\max}(\mathbf{A}_i) > 0$, therefore, the right-inequality of (15) holds. From Eq. (10) and the left-inequality of (15), we have

$$T \leq c_3|\lambda_{\min}(\mathbf{A}_3)|\,\|\mathbf{u}\|^2 = -c_3\lambda_{\min}(\mathbf{A}_3)\|\mathbf{u}\|^2$$

that is, in this case,

$$T_{\sup}|_{T_3<0} = c_3|\lambda_{\min}(\mathbf{A}_3)|\,\|\mathbf{u}\|^2 = -c_3\lambda_{\min}(\mathbf{A}_3)\|\mathbf{u}\|^2 \qquad (17)$$

To summarize cases I and II,

$$T_{\sup}|_{T_3\neq 0} = c_3|\lambda^*(\mathbf{A}_3)|\,\|\mathbf{u}\|^2 \qquad (18)$$

where

$$\lambda^*(\mathbf{A}_3) = \lambda_{\max}(\mathbf{A}_3)\mu(T_3) + \lambda_{\min}(\mathbf{A}_3)\mu(-T_3)$$

and $\mu(\bullet)$ is a unit step function.

It can be shown by similar derivation that when T_i (i =1,2,3) is chosen to be the non-zero component in formulating the magnitude and the direction constraints of the torque in spherical coordinates, the potential maximum torque output

$$T_{\sup}|_{T_i\neq 0} = c_i|\lambda^*(\mathbf{A}_i)|\,\|\mathbf{u}\|^2$$

where

$$\lambda^*(\mathbf{A}_i) = \lambda_{\max}(\mathbf{A}_i)\mu(T_i) + \lambda_{\min}(\mathbf{A}_i)\mu(-T_i)$$

$$c_i \triangleq \frac{1}{2}\sqrt{a_i^2 + b_i^2 + 1} > 0$$

a_i and b_i are defined by Eqs (6), (7), and the following equations:

$$a_2 = \cot\vartheta, \quad b_2 = \cot\varphi/\sin\vartheta$$
$$a_1 = \tan\vartheta, \quad b_1 = \cot\varphi/\cos\vartheta$$

Taking into account of all the three possibilities of choosing T_i(i = 1,2,3) in formulating the magnitude and the direction constraints of the torque, the maximum torque potential then becomes

$$T_{\sup} = \min_i \{T_{\sup}|_{T_i\neq 0}\} = \min_i \{c_i|\lambda^*(\mathbf{A}_i)|\}\|\mathbf{u}\|^2 \qquad (19)$$

where i = 1,2,3.

Several remarks should be made about the maximum torque formula, Eq. (19).

Remark 1. The $T_{\sup}/\|\mathbf{u}\|^2$ is a function of the torque direction variables and the rotor orientation. Unlike the 1-DOF devices, the output torque of a 3-DOF motor is direction-varying and orientation-dependent.

Remark 2. From Eq. (19), we conclude that in a given torque directon at a certain rotor orientation, the maximum torque output capacity is directly proportional to the input electrical power, that is,

$$\|\mathbf{u}\|^2 \uparrow \Rightarrow T_{\sup} \uparrow \text{ or } \|\mathbf{u}\|^2 \downarrow \Rightarrow T_{\sup} \downarrow$$

which physically makes sense. Equation (19) also indicates that the maximum torque output and the minimum power input are competing requriements. Therefore, a tradeoff between these two is necessary in control strategy development.

Remark 3. Unlike the conventional three-consecutive-rotational-joint motor system which typically uses three 1-DOF motors in the x, y, and z directions to realise three-dimensional motion, the current loads of the spherical motor can be distributed among m(>3) coils due to the multiple choices of the control vector. This will reduce the load on each coil and hence the heat dissipation. In other words, for a same power input, the 3-DOF motors can generate larger torque output than the 1-DOF motors.

Remark 4. In order to have a larger isotropic output torque capacity while the power consumption is kept the same, it is more desirable that the motor (structure and parameters) is designed such that $\lambda_{max}(\mathbf{A}_i) = -\lambda_{min}(\mathbf{A}_i)$.

4. Applications of the Maximum Torque Formula

The maximum torque formula, Eq. (19), can be applied to characterise and optimise the VR spherical motor. Four typical applications are discussed in the following subsections.

4.1. Payload Evaluation of the VR Spherical Motor

Payload is one of the important specifications in characterising a motor. Payload determination for the VR spherical motor is essentially a minimax problem, namely, the evaluation of the minimum T_{sup} over the whole torque space and the entire orientation space. Theoretically, the payload of a VR spherical motor can be calculated by using the maximum torque formula, Eq. (19). The main difficulty of the evaluation in practice, however, is that the computation is very numerically demanding, since both torque and rotor orientation spaces must be searched. The torque space denoted by $\mathbf{T}$ is determined by $0 \le \vartheta \le 2\pi$ and $0 \le \varphi \le 2\pi$, while the rotor orientation space represented by $\mathbf{O}$ is given in terms ZYZ Euler angles by $0 \le \psi \le 2\pi$, $0 \le \theta \le \pi/4$, and $0 \le \phi \le 2\pi$. If the partition resolution of the torque and rotor orientation spaces is r points/radian, the number of points (steps) where the possible maximum torque output need to be computed is $4 \times (\pi r)^5$. If an Intel IBM PC 486 (25 MHz) is used, and the computation time for each point (step) is 200 ms (from simulation), the total computation time would be $800 \times (\pi r)^5$ ms. Even for a one-degree partition ($r = 180/\pi$), the computation would take 4793 years; such an undertaking is far beyond the computing environment used for this research. In order to overcome the computational problem in characterising a motor, two approaches, namely elimination of the torque direction variables in the torque space and use of the geometric (structural) symmetry of the rotor orientation space, will be used in determining the payload.

4.1.1. *Elimination of Torque Direction Variables in the Torque Space*

As we shall see, the torque direction variables appear as bounded functions in the maximum torque formula; therefore the torque direction variables can be eliminated explicitly from the formula by means of minimisation. This will significantly reduce the computation, hence improve the computational efficiency.

By substituting c_3 in terms of φ and ϑ using Eqs (11), (6), and (7) into Eq. (18), we have

$$\left.\frac{T_{sup}}{\|\mathbf{u}\|^2}\right|_{T_3\neq 0} = \frac{1}{2}[(\tan\varphi\cos\vartheta)^2 + (\tan\varphi\sin\vartheta)^2 + 1]^{\frac{1}{2}}|\lambda^*(\mathbf{A}_3)| = \frac{|\lambda^*(\mathbf{A}_3)|}{2|\cos\varphi|}$$

Since $|\cos\varphi| \le 1$, therefore

$$\left.\frac{T_p}{\|\mathbf{u}\|^2}\right|_{T_3\neq 0} = \min_{\mathbf{T}_3\cup\mathbf{O}}\left\{\left.\frac{T_{sup}}{\|\mathbf{u}\|^2}\right|_{T_3\neq 0}\right\} = \min_{\mathbf{O}}\left\{\frac{1}{2}|\lambda_3^*|\right\} \tag{20}$$

where $T_p/\|\mathbf{u}\|^2$ denotes the payload to input power ratio, and $|\lambda_i^*| = \min\{|\lambda_{min}(\mathbf{A}_i)|, |\lambda_{max}(\mathbf{A}_i)|\}$.

It has been shown in Section 3.3 that

$$T_{sup}|_{T_2\neq 0} = c_2|\lambda^*(\mathbf{A}_2)|\,\|\mathbf{u}\|^2$$

when $T_2(\neq 0)$ is chosen as the non-zero component in the maximum torque formulation of the constraints and the objective function. Furthermore,

$$\left.\frac{T_{sup}}{\|\mathbf{u}\|^2}\right|_{T_2\neq 0} = \frac{1}{2}\left[\left(\frac{\cot\varphi}{\sin\vartheta}\right)^2 + \left(\frac{\cos\vartheta}{\sin\vartheta}\right)^2 + 1\right]^{\frac{1}{2}}|\lambda^*(\mathbf{A}_2)| = \frac{|\lambda^*(\mathbf{A}_2)|}{2|\sin\varphi\sin\vartheta|} \tag{21}$$

Since $|\sin\varphi\sin\vartheta| \le 1$, therefore

$$\left.\frac{T_p}{\|\mathbf{u}\|^2}\right|_{T_2\neq 0} = \min_{\mathbf{T}_2\cup\mathbf{O}}\left\{\left.\frac{T_{sup}}{\|\mathbf{u}\|^2}\right|_{T_2\neq 0}\right\} = \min_{\mathbf{O}}\left\{\frac{1}{2}|\lambda_2^*|\right\}$$

Similar to the case $T_2 \neq 0$, when T_1 ($\neq 0$) is chosen to be the non-zero component in formulating the constraints and the objective function of the maximum torque formulation, we have the following results:

$$\left.\frac{T_{sup}}{\|\mathbf{u}\|^2}\right|_{T_1\neq 0} = c_1|\lambda^*(\mathbf{A}_1)| = \frac{1}{2}\left[\left(\frac{\cot\varphi}{\cos\vartheta}\right)^2 + \left(\frac{\sin\vartheta}{\cos\vartheta}\right)^2 + 1\right]^{\frac{1}{2}}|\lambda^*(\mathbf{A}_1)| = \frac{|\lambda^*(\mathbf{A}_1|}{2|\sin\varphi\cos\vartheta|} \tag{22}$$

and

$$\left.\frac{T_p}{\|\mathbf{u}\|^2}\right|_{T_1\neq 0} = \min_{\mathbf{T}_1\cup\mathbf{O}}\left\{\left.\frac{T_{sup}}{\|\mathbf{u}\|^2}\right|_{T_1\neq 0}\right\} = \min_{\mathbf{O}}\left\{\frac{1}{2}|\lambda_1^*|\right\}$$

To summarise,

$$\frac{T_p}{\|\mathbf{u}\|^2} = \min_{\mathbf{T}\cup\mathbf{O}}\left\{\frac{T_{sup}}{\|\mathbf{u}\|^2}\right\} = \min_{\mathbf{O}}\left\{\frac{1}{2}|\lambda_1^*|,\frac{1}{2}|\lambda_2^*|,\frac{1}{2}|\lambda_3^*|\right\} \tag{23}$$

where

$$|\lambda_i^*| = \min\{|\lambda_{min}(\mathbf{A}_i)|, |\lambda_{max}(\mathbf{A}_i)|\} \quad (i = 1,2,3)$$

Note that $\mathbf{T}_i$ (i = 1,2,3) is a subset (subspace) of $\mathbf{T}$ corresponding to $T_i \neq 0$, and $\mathbf{T} = \mathbf{T}_1 \cup \mathbf{T}_2 \cup \mathbf{T}_3$. Since Eqs (20), (21), and (22) are even functions with respect to ϑ and φ, the torque space for calculating $T_p/\|\mathbf{u}\|^2$ can be reduced to $0 \leq \varphi \leq \pi$ and $0 \leq \vartheta \leq \pi$. Furthermore, by eliminating the torque direction variables the amount of computation for $T_p/\|\mathbf{u}\|^2$ is reduced to $1/(2\pi r)^2$ of the original amount. For example, if r is chosen to be $180/\pi$ radians (1°), then the amount of computation will be reduced 1.296×10^5 times by the elimination of torque direction variables.

4.1.2. Use of Geometric (Structural) Symmetry of the Rotor Orientation Space

After the elimination of the torque direction variables, the formula for calculating the payload is only a function of rotor orientations. The payload computation can be further reduced by considering the geometric (structural) symmetry of the motor. Using the symmetry, the orientation space for calculating the payload is reduced to $\mathbf{O}_s$, $0 \leq \psi \leq 2\pi/5$, $0 \leq \theta \leq \pi/4$, and $0 \leq \phi \leq \pi/2$ [4]. Therefore, the payload computation is further reduced to 1/20 of the amount after the elimination of the torque direction variables.

Accounting for both the torque direction variable elimination and the use of structural symmetry, the computation time for payload evaluation is finally reduced to $10(\pi r)^3$ ms. As an example, for the one degree ($r = 180/\pi$) partition, the time will be approximately 16 h if the IBM PC 486 is used, which is quite acceptable in practice.

4.2. Numerical Verification of the Non-Singularity Property

One of the important criteria in designing a 3-DOF motor is the non-singularity property, i.e. the motor should be able to generate certain torque in all directions at any rotor orientation within the workspace. Although this characteristic has been claimed for the VR spherical motor, neither theoretical nor experimental (numerical) proof has been given to support the claim. With the aid of the analytical payload evaluation formula, Eq. (23), and the numerical techniques developed in Section 4.1, we are able to prove numerically the non-singularity property of the VR spherical motor.

Since the torque model of the VR spherical motor is in quadratic form, the non-singularity property requires that $\mathbf{A}_i$ (i = 1,2,3) be indefinite, namely, $\lambda_{min}(\mathbf{A}_i) < 0$ and $\lambda_{max}(\mathbf{A}_i) > 0$. Therefore, from Eq. (23), we have

$$\frac{T_p}{\|\mathbf{u}\|^2} = \min_{\mathbf{T}\cup\mathbf{O}}\left\{\frac{T_{sup}}{\|\mathbf{u}\|^2}\right\} = \min_{\mathbf{O}_s}\left\{\frac{1}{2}|\lambda_1^*|,\frac{1}{2}|\lambda_2^*|,\frac{1}{2}|\lambda_3^*|\right\} > 0$$

which indicates that the motor can output a non-zero torque in all directions at any rotor orientation. By verifying the signs of $\lambda_{min}(\mathbf{A}_i)$ and $\lambda_{max}(\mathbf{A}_i)$ (i = 1,2,3) at any rotor orientation in the payload evaluation, it can be proved numerically that the number of singular points of the VR spherical motor is zero.

4.3. Design (Structure and Parameters) Optimisation

4.3.1. Characteristic Orientation

Optimisation often plays an important role in design and manufacturing of a VR spherical motor. A successful design optimisation will improve the performance of the system, provide better insight into potential applications, and aid in developing future motor designs. One of the fundamental differences between 3-DOF and 1-DOF motors is that the output torque of the former is direction-varying and orientation-dependent. This unique feature of 3-DOF motors leads to a significant difference in characterisation and optimisation. In particular, in design optimisation the characteristic orientation at which the motor parameters are optimised, needs to be taken into consideration, which is not necessary in the 1-DOF case. The characteristic orientation should be the position where the motor has the minimum torque output capacity, that is where the maximum payload of the motor is determined. The determination of the characteristic orientation is essential, since global design optimisation can only be obtained at that orientation. The characteristic orientation can be determined by tracking the rotor orientation while the payload-to-input power ratio is evaluated.

4.3.2. Objective Function (Optimisation Criterion)

To design optimally a VR spherical motor with uniform torque characteristics, the objective function should be chosen to meet the following requirements: (1) the objective is independent of the electrical inputs; and (2) the minimum torque output capacity over the torque and orientation spaces is maximised. The explicit formula for evaluating the payload-to-input power ratio, Eq. (23), provides such a formulation, namely

$$J = \max \{T_p/\|\mathbf{u}\|^2\} = \max \left\{ \min_{O_s} \left\{ \frac{1}{2}|\lambda_1^*|, \frac{1}{2}|\lambda_2^*|, \frac{1}{2}|\lambda_3^*| \right\} \right\}$$

Such an objective function, associated with certain constraints [2], forms a maximum torque formulation for design optimisation. The results (optimal geometric parameters) of the system will ensure the uniform torque characteristics and guarantee a maximum torque output capacity for the particular configuration.

4.4. Optimal Solution to the Maximum Torque Formulation

The maximum torque formula, Eq. (19), states that the maximum torque output of the VR spherical motor is always bounded. The actual maximum torque output and the corresponding optimal control inputs can be further obtained by solving the original optimisation problem formulated in Section 3.2. There is, however, no closed form solution to the problem in general. To solve for the optimal control inputs, various numerical techniques can be used. A typical example is the generalised reduced gradient (GRG) method [5]. It has been found numerically that the GRG method works well in solving the optimisation problem off-line. For real-time implementation, a small lookup table compiled off-line and an optimal on-line estimation algorithm can be employed [4].

5. Results and Discussion

A computer simulation has been carried out, based on Eq. (23), to compute the maximum payload-to-input power ratio, the corresponding characteristic orientation, and the number of singular points. The following is part of the printed results.

> The payload-to-input power ratio is 0.057007 $\times 10^{-6}$ Nm/(amper–turns)^2.
>
> The corresponding characteristic orientation in degrees is $\psi = 8$, $\theta = 32$, and $\phi = 39$.
> The number of singular points is 0.

Table 1. Theoretical and actual payloads at the characteristic orientation.

$\|\mathbf{u}\|^2$	11	44	99	176
T_p	0.6271	2.5083	5.6437	10.0332
$\hat{T}_p$	0.6197	2.4788	5.5773	9.8712

$\|\mathbf{u}\|^2$ in 10^6 (ampere–turns)^2, T_p and $\hat{T}_p$ in Nm.

Using the payload-to-input power ratio obtained in the simulation, absolute payload values of T_p representing the output torque capacity can be calculated by specifying $\|\mathbf{u}\|^2$. Some of the typical values are listed in Table 1. For example, one observes from Table 1 that if $\|\mathbf{u}\|^2$ is specified as 44 $\times 10^6$ (ampere–turns)^2, then the maximum payload of the motor is approximately 2.5083 Nm.

Also listed in Table 1 is the actual maximum torque output at the characteristic orientation in a specified direction $\varphi = 0$ or π, $\hat{T}_p$. The corresponding optimal control inputs are given in Table 2. The optimal control inputs and the maximum torque output are computed using an off-the-shelf GRG optimisation package with a 10^4 ampere–turns input limit to each coil and a constraint tolerance of 10^{-4}.

The theoretical and actual payload values are plotted in Fig. 4. From Table 1 and Fig. 4, one observes that when the power consumption is small, the actual maximum torque output is close to the theoretically predicted superior limit. But the error becomes larger when the power input goes higher. This is due to the fact that when the electrical input power is high, the inputs (e.g. currents) to stator coils become large, which causes the magnetic

Table 2. Optimal control inputs at the characteristic orientation.

$\|\mathbf{u}\|^2$	11	44	99	176
u_1	0.1399	0.2789	0.4197	−0.4264
u_2	−0.9072	−1.8144	−2.7216	3.2994
u_3	2.6876	5.3751	−4.4569	7.0061
u_4	0.1441	0.2883	0.4324	−0.5333
u_5	−0.1628	−0.3256	−0.4883	0.3203
u_6	0.1462	0.2925	0.4387	−0.4536
u_7	−0.7796	−1.5592	−2.3389	3.6355
u_8	−1.4857	−2.9713	8.0627	−9.9999
u_9	0.1441	0.2883	0.4324	−0.5333
u_{10}	−0.0811	−0.1623	−0.2435	−1.2327
u_{11}	0.1544	0.3089	0.4633	−0.4909

$\mathbf{u}$ in 10^3 (ampere–turns).

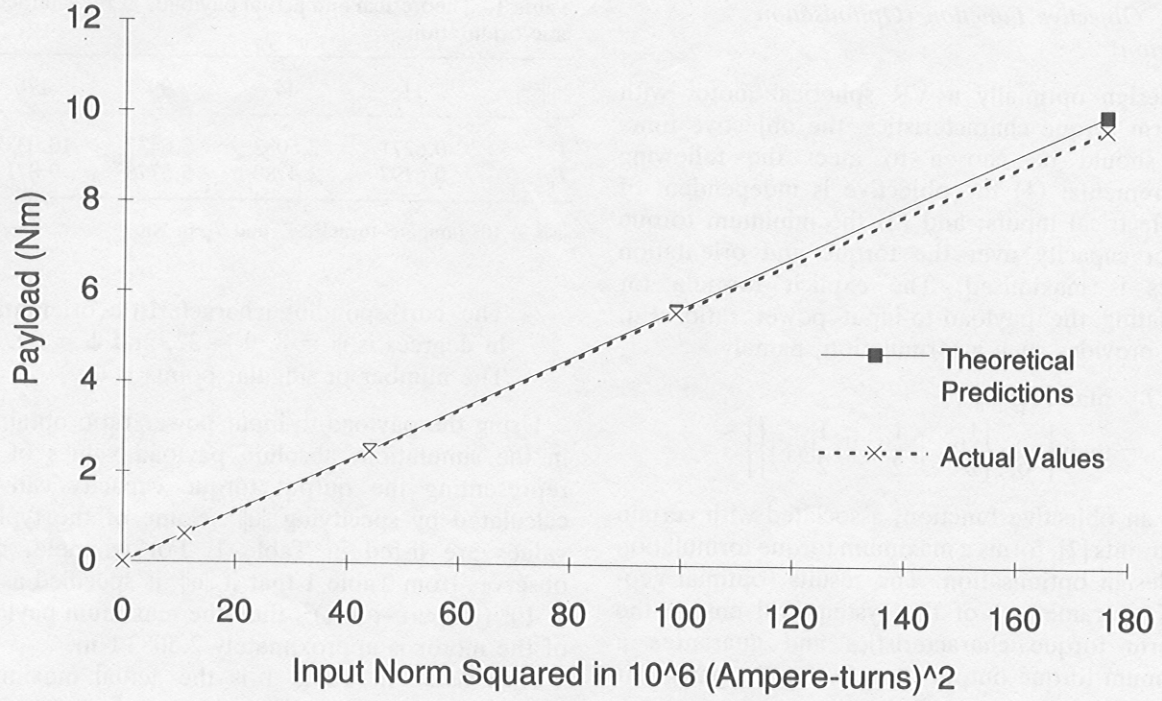

Fig. 4. Characteristic curves – maximum torque *vs*. power input.

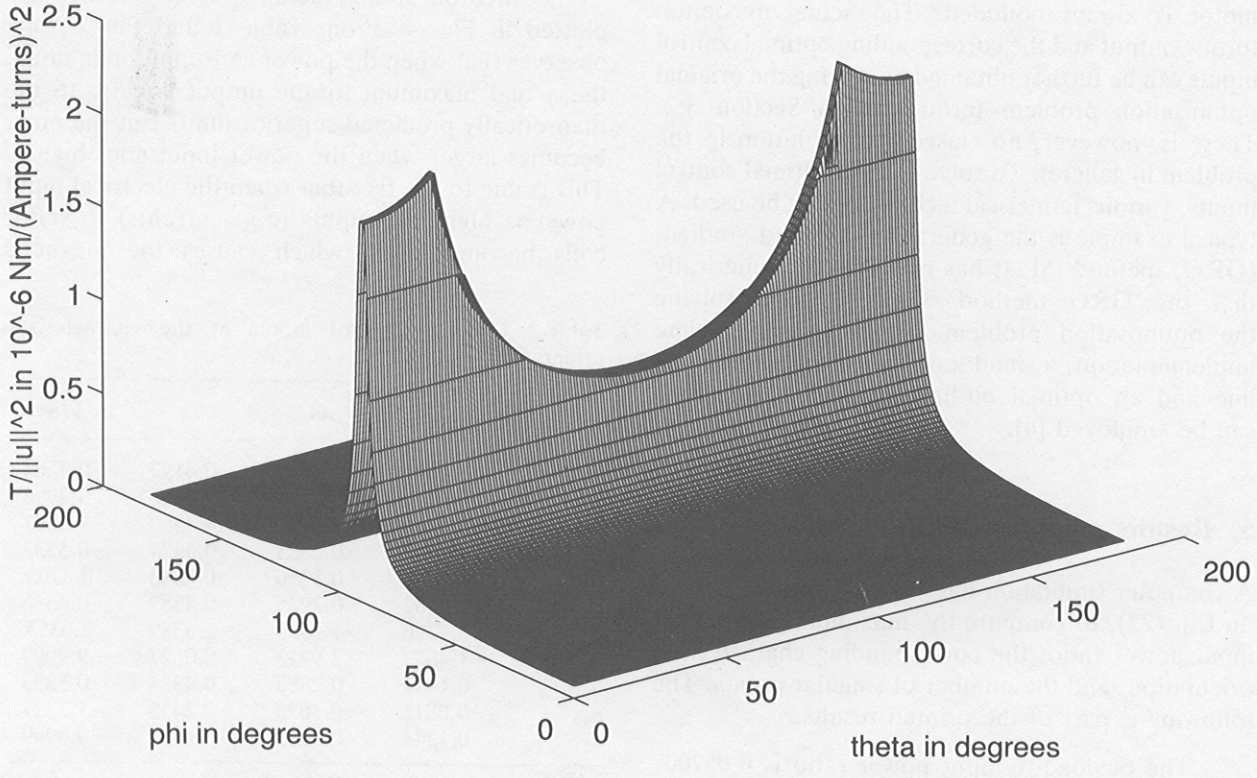

Fig. 5. Torque profile – maximum torque-to-input power ratio *vs* direct variables.